Silicon (2024) 16:45–59
https://doi.org/10.1007/s12633-023-02648-4

RESEARCH

Fabrication and Mechanical Characterization of Al-Zn-Cu Alloy /SiC/ TiB_2 Hybrid Reinforced Metal Matrix Composite using Top Loaded Bottom Pouring Stir Casting Method

Nitish Kumar Singh[1] · **S. Balaguru**[1]

Received: 28 June 2023 / Accepted: 26 August 2023 / Published online: 5 September 2023

Abstract
In this study, AA7075/SiC/TiB_2 hybrid composites were fabricated using the top-loaded bottom-pouring stir-casting route. The primary reinforcement, silicon carbide (SiC), and the secondary reinforcement, titanium diboride (TiB_2), were used in weight percentages of 0–12% and 3%, respectively. The effect of reinforcement addition on the microstructure, physical, mechanical, and tribological properties of the hybrid composites was investigated using a Scanning Electron Microscope (SEM) with Energy Dispersive X-ray (EDX), as well as tensile, compression, hardness, and wear testing machine. The results showed that the addition of SiC and TiB_2 reinforcement materials can significantly enhance the ultimate tensile strength, yield strength, compressive strength, and hardness of the hybrid composite, with a maximum increment of 21.86%, 20.33%, 46.32%, and 32.56%, respectively, compared to unreinforced AA7075 alloy. The microstructure results indicated a homogeneous particle dispersion in the molten matrix. The SiC and TiB_2-reinforced AA7075 matrix composites present an excellent choice for automotive, aerospace, and marine applications.

Keywords AA7075 · Stir casting · Silicon carbide · Titanium di-boride · Mechanical properties · Hybrid composite

1 Introduction

The rich availability, around 8% of the mass of our earth's crust, is aluminium, making it the third most useful material after silicon and oxygen [1]. Currently, lightweight materials are in higher demand in the aircraft and vehicle industries [2]. Recent years have seen a lot of interest in aluminium and composites due to their low density and unique characteristics, including high strength, damping capacity, and wear resistance [3]. The wide use of aluminium metal matrix composites in aerospace, automobile, structural, and naval engineering has established them as a new class of engineering materials [4]. To improve its mechanical and tribological properties, researchers have added numerous reinforcements (particles) to the base metal [5, 6]. There are several techniques to make aluminium metal matrix composites, including stir casting [7, 8], powder metallurgy, hot forging [9], friction stir processing [10, 11], sintered through conventional technique [12] and squeeze casting [13]. Stir casting is generally preferred over other manufacturing processes for fabricating aluminium hybrid reinforced composites [14, 15]. This method offers ease of production and is an economical way to prepare composites [16]. For this reason, stir casting has been used in current research to fabricate hybrid composites. This technique's wettability of reinforcements with the matrix alloy is a critical challenge. Calcium powder was used as a viscosity-enhancing agent, as well as silicon carbide (SiC), and titanium diboride (TiB_2) as a reinforcing agent, which helped improve aluminum reinforcement's wettability. Extensive research has been conducted to investigate the physical and mechanical properties of composites comprising various aluminum series and reinforcement materials. All aluminum series have different strengths, but AA7075 is the strongest and has the greatest potential for dry sliding wear applications [17]. AA7075 exhibits the greatest strength, hardness, and lowest wear rate among all aluminum series, including 1XXX, 2XXX, 3XXX, 6XXX, and 7XXX. A low weight-to-strength ratio, excellent wear resistance, and low creep resistance make it an excellent choice for automobiles, aerospace, sports, and electronics

✉ S. Balaguru
balaguruiitm@gmail.com

[1] School of Mechanical Engineering, VIT Bhopal University, Sehore, Madhya Pradesh, 466114, India

Table 1 Properties of matrix and reinforcement material

	Matrix material (AA7075) [17, 23]	Reinforcement material	
		SiC [6, 18, 23, 25, 26]	TiB_2 [4, 6, 23]
Density (g/cm^3)	2.81	3.21	4.52
Melting point	470–550 °C	2730 °C	2790 °C
Modulus of elasticity (GPa)	71.7	400–500	530
Poisons ratio	0.33	0.14	0.1–0.15
Hardness		2,300–2,850 HV	960 HV
Tensile strength (MPa)	230 MPa		3900
Yield strength	105 MPa		

applications [18, 19]. This study uses silicon carbide (SiC) as a primary reinforcement and titanium-diboride (TiB_2) as a secondary reinforcement. The chemical compatibility of SiC with aluminium allows it to form a strong bond with the matrix [20–22]. TiB_2 possesses outstanding properties such as its high melting point at 3,230 °C, its high hardness (960 HV), its high elastic modulus (530 GPa), and its superior thermal stability [23, 24]. Because of their outstanding qualities, SiC and TiB_2 are excellent choices for primary and secondary reinforcement for advanced applications in automotive, weaponry, aviation, and aerospace. Parts which are used in automotive, weaponry, aviation, and aerospace subjected to extremely high temperatures which require strong abrasion resistance. In such type of advanced application applications SiC and TiB_2 are excellent choices for primary and secondary reinforcement because of their outstanding properties. Properties of matrix and the used reinforcement particles are included in Table 1.

Many authors reported the effect of reinforcement on the properties of different aluminium series. Still, to our knowledge, no systematic research has been done to investigate how SiC and TiB_2 concentration affect the physical, microstructural, mechanical, and tribological behavior of the AA7075 composite. The prime objective of this investigation is to fabricate and study the effect of varying wt.% of SiC and TiB_2 on the physical, microstructural, mechanical, and tribological properties of AA7075/SiC/TiB_2 hybrid composites. In the present work, different weight % of SiC (3, 6, 9, and 12 wt. %) and 3 wt. % of TiB_2 particles have been added to the synthesis AA7075/SiC/TiB_2 hybrid composites by top loaded bottom pouring stir casting method. Microstructure, physical properties (theoretical, actual density and porosity), Mechanical properties (yield strength, ultimate tensile strength, percentage of elongation, compressive strength and hardness) and tribological properties were analyzed.

This article has the following structure. Section 1 discusses the introduction of composite material with research gap identified. Section 2 explains the details procedure of experimental analysis i, e material fabrication, microstructural, and mechanical characteristics. Section 3 describes the result and discussion i, e effect of various parameters on the mechanical characteristics of aluminium hybris composites. Section 4 concludes this paper.

2 Experimental Details

2.1 Materials

In this study, the researchers utilized the 7075 Al alloy as the matrix metal due to its extensive application in various industrial sectors, including automotive, aerospace, marine, construction, and outdoor environments [27]. Additionally, its suitability for ageing heat treatment made it readily accessible [28–30]. Table 2 depicted the chemical composition of the matrix material, which was obtained using energy dispersive spectroscopy (EDS) conducted on a scanning electron microscope (SEM). AA7075/SiC/TiB_2 hybrid composite was created using different weight percentages of SiC (3%, 6%, 9%, and 12%) while maintaining a constant weight percentage of TiB_2 at 3%, as shown in Table 3. The presence of TiB_2 particles improved the tribological and hardness characteristics of the composite while maintaining excellent chemical bonding and stability [31]. Hence, the weight percentage of TiB_2 remains unchanged. khairakdien et al. [32] examined the influence of SiC reinforcement on aluminium matrix and noticed that increasing the weight percentage of SiC beyond 15 wt. % resulted in a significant decrease in strength. Therefore, to ensure that the reinforcement weight percentage remains below 15 wt.%, the weight

Table 2 Chemical composition of AA7075

Element	Cu	Mg	Al	Si	Ca	Mn	Fe	Zn
Weight %	2.1	3.81	86.18	0.75	0.06	0.82	0.76	5.52

Table 3 Composition of fabricated aluminium matrix (AA7075) hybrid composite

Sample	Matrix AA7075 wt. %	Reinforcement	
		SiC wt. %	TiB_2 wt. %
S-1	100	0	0
S-2	96	3	3
S-3	91	6	3
S-4	88	9	3
S-5	85	12	3

percentage of SiC was varied as follows: 0%, 3%, 6%, 9%, and 12%, respectively.

2.2 Material Synthesis

Hybrid aluminum AA7075 metal matrix composites were fabricated using the top-loaded bottom-pouring stir-casting furnace shown in Fig. 1. Initially, aluminium alloy AA7075 was taken in the crucible placed in a top-loaded bottom-pouring stir casting furnace and melted at 750 °C. To eliminate volatile substances and reduce temperature differentials between the molten metal and reinforcement particles, the SiC (particle size: 25 µm) and TiB_2 (particle size: 15 µm) reinforcements were placed in a separate muffle furnace and preheated at 450 °C. After the melting of the AA7075 alloy, the temperature of the stir-casting furnace was raised from 750 °C to 900 °C. After that vortex formation was achieved by stirring molten metal at 350–450 revolutions per minute using a graphite impeller. The preheated (450 °C) SiC and TiB_2 particles were fed into the molten metal by using the feeder. After adding the reinforcement particles completely, the melt was mechanically stirred at 500–550 rpm until completely incorporated. Stirring was continued for 5 min to ensure better distribution. Sahu et al. [19] suggested the above optimal stirring process parameter for AA7075 alloy. A thoroughly mixed melt was put in to preheat the graphite-coated cast iron finger dies shown in Fig. 2 (a). Finally, the solidified cast melt was removed from the die, as depicted in Fig. 2(b).

2.3 Density

After the fabrication of the hybrid composite, the sample was cut through the machining process. The density of matrix (AA7075) and reinforcement SiC and TiB_2 are 2.81 g/cm^3, 3.21 g/cm^3 and 4.52 g/cm^3, respectively. The rule of mixture calculated the theoretical density of hybrid composites by using Eq. 1 [33]. The fabricated composites' experimental density was evaluated using Archimedes' principle the detailed procedure for evaluating the density has been described in our previous work [34]. The porosity of the fabricated composite was calculated by using Eq. 2 [35].

$$\rho_t = \frac{1}{\frac{Wt_{r1}}{\rho_{r1}} + \frac{Wt_{r2}}{\rho_{r2}} + \frac{Wt_m}{\rho_m}} \tag{1}$$

where, Wt_{r1},Wt_{r2}, and Wt_m represents the weight percentage of reinforcement 1 (SiC), reinforcement 2 (TiB_2) and matrix material (AA7075), respectively. ρ_{r1},ρ_{r2}, and ρ_m represents the theoretical density of reinforcement 1 (SiC), reinforcement 2 (TiB_2) and matrix material (AA7075), respectively.

$$Porosity(\%) = \frac{\text{Theoretical Density-Actual Density}}{\text{Theoretical Density}} \times 100 \tag{2}$$

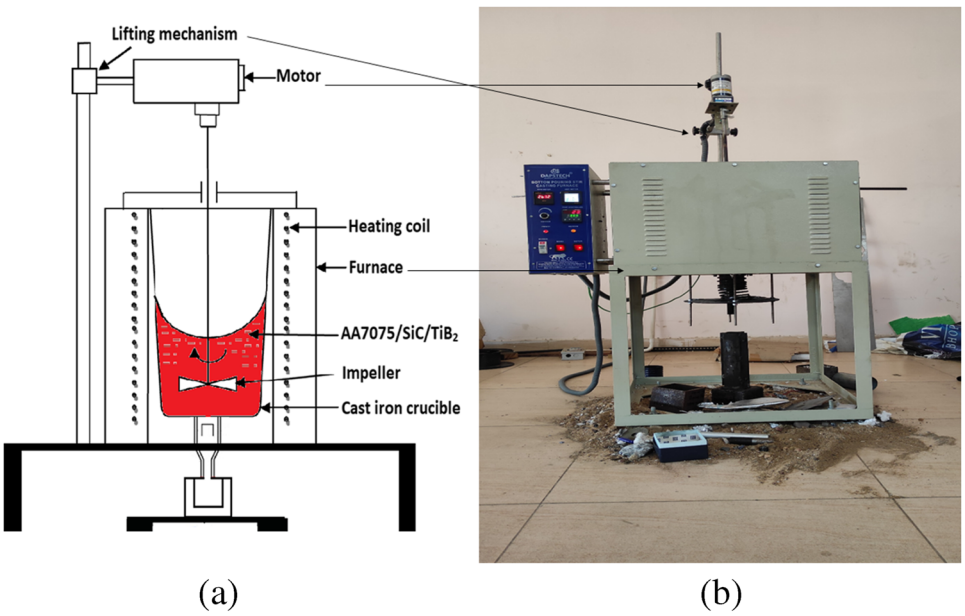

Fig. 1 Top loaded bottom pouring Stir casting Furnace (**a**) schematic view (**b**) real view

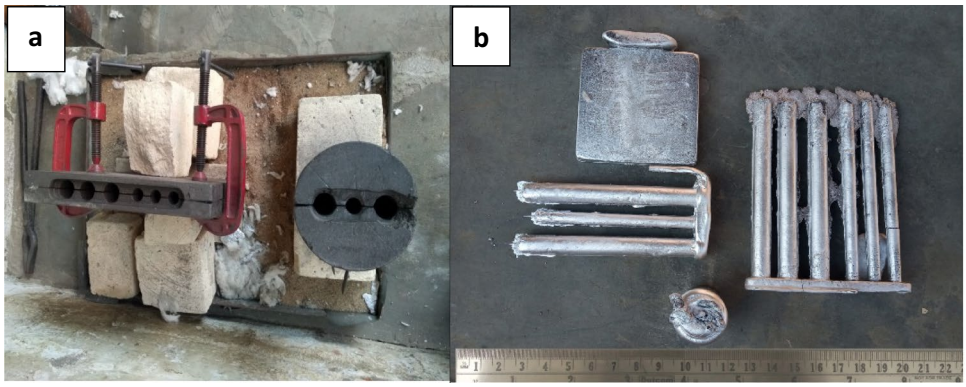

Fig. 2 Furnace used for making hybrid composite (**a**) graphite-coated cast iron finger dies (**b**) Casted specimens

2.4 Mechanical Properties

The prepared aluminium hybrid composite (AHCs) AA7075/xSiC/3 wt. % TiB_2 and AA7075 alloy were examined for mechanical behavior employing tensile properties, compressive properties, and hardness properties. The tensile specimen was prepared according to the ASTM E8 standard shown in Fig. 3 with a gauge diameter of 12 mm and a gauge's length of 70 mm. At room temperature, the UTE/C-400 universal testing machine was used to conduct tensile and compressive tests at a strain rate of 0.01/S. Rockwell hardness tests were conducted on the prepared samples using a Rockwell hardness machine (FIE make Model IRB-250). For the hardness test, an indenter with a 1/16 diamond ball and a 100 Kgf load was used to indent the surface of the hybrid composite. Three locations were indented, and average values were reported to ensure accuracy.

2.5 Wear Test

Both unreinforced and reinforced hybrid composite specimens were subjected to dry sliding wear tests on the pin-on-disc wear testing equipment TR-20LE per ASTM G99 [36] requirements. Before the wear test, all the specimens were polished with 1200 and 1500-grit emery paper. Both unreinforced and reinforced hybrid composite specimens were subjected to dry sliding wear tests on the pin-on-disc wear testing equipment TR-20LE per ASTM G99 [32]. SISI EN 32 steel disk was used as a counter surface, and pin (Sample) with the dimensions of 10 mm diameter and 30 mm

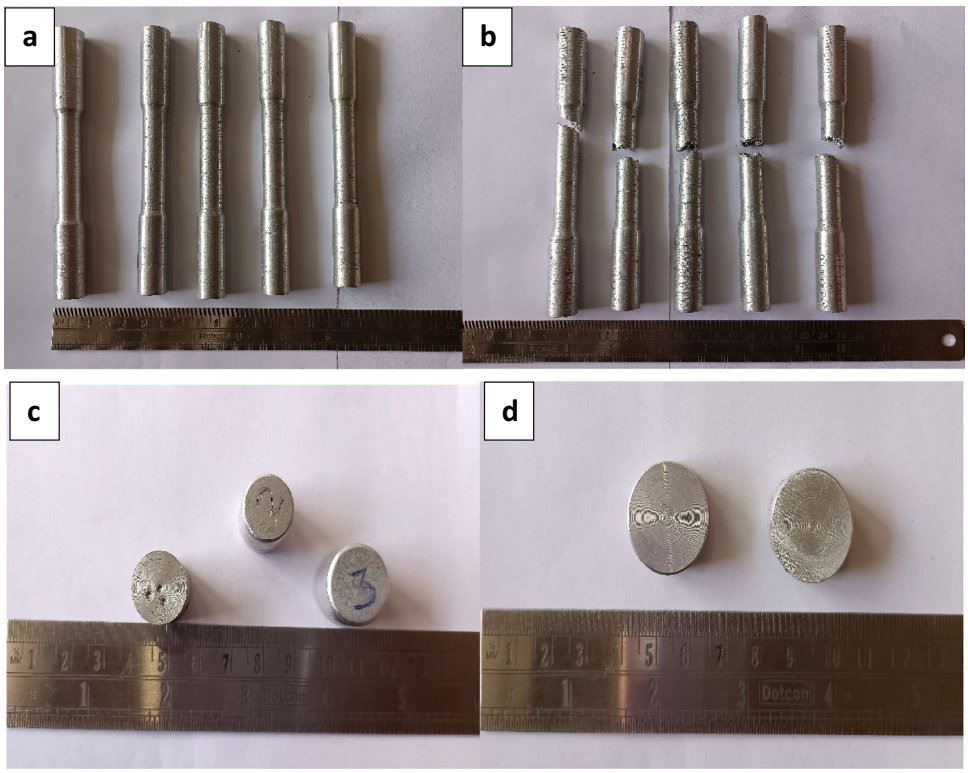

Fig. 3 Test samples (**a**) tensile before the test (**b**) tensile after the test (**c**) compressive (**d**) hardness

length are used to examine the wear behavior. wear test has been carried out in two different conditions such as (i) varying sliding distance (1000 to 5000 m) at an applied load of 2 kg and sliding velocity of 1.7 m/s, and (ii) varying loads (2–6 kg) with sliding distance 1000 m. For all test samples wear track diameter is taken as 100 mm. While experimenting before and after each test the weight of the specimens was measured using an electronic weighing Machine with a precision of 0.001 mg. Equation 3 was used to compute the wear rate for all samples [37].

$$Wear\ rate(mm^3/m) = \frac{weight\ loss(gm)}{Density(g/mm^3) * Sliding\ distance(m)} \quad (3)$$

2.6 Microstructural Test

The samples were polished and etched using standard metallographic techniques to examine their microstructure. In the first step, the hybrid composite specimens were cut into small pieces on a lathe. Subsequently, the samples underwent a coarse grinding process using emery paper with grit sizes of 60 and 80. The objective of coarse grinding is to create an initial flat surface for further grinding. Following coarse grinding, the samples were cleaned using alcohol. Subsequently, medium and fine grinding were performed using 320 grit emery paper to achieve a surface free of scratches. After grinding, the samples were polished by applying diamond paste onto a velvet cloth, which was rotated at 200 rpm for 5-min intervals until a mirror-like surface was achieved. This polishing process was carried out using a Modern-1 Double Disc Grinder/Polisher machine. Subsequently, etching was performed using Keller's etchant for a duration of 20–50 s as per our previous study [38]. The energy-dispersive X-ray spectroscopy (EDS) technique analyzes samples' chemical and elemental composition. The main principle of spectroscopy is based on the unique atomic structure of every element. The present study used a scanning electron microscope (ZEISS EVO 18) to perform EDS on the sample microstructure. At different portions of a sample, EDS analysis was performed.

3 Result and Discussion

3.1 Density and Porosity

Figure 4 shows the theoretical and experimental densities of the AA7075 alloy (unreinforced) and AA7075/SiC/TiB_2 hybrid composites. The Archimedes principle was used to calculate the samples' experimental densities. The experimental density of the samples obtained in the range of 2.768–2.815 g/cm^3 for AA7075 matrix alloy with the 0–12 wt. % of SiC and 3 wt. % of TiB_2 respectively. The samples' theoretical density was evaluated using Eq. 1 and calculated ranging from 2.81–2.909 g/cm^3 for AA7075 matrix alloy with the 0–12 wt. % of SiC and 3 wt. % of TiB_2 respectively. Due to manufacturing defects involved with casting, experimental density has been affected even with calcium added to the melt as wetting agents. The samples exhibit porosity, shrinkages, and slag inclusions due to the high temperature used to make the molten metal. Several factors caused the rise in porosity in the composites. In the aluminium matrix, reinforcement particles are distributed homogeneously by stirring. This process also controls the accumulation of particles while increasing reinforcement contents; as a result of this stirring process, gas is introduced into the molten metal. The gas entrapped during solidification caused porosity. Based on previous studies, the developed reinforced composites are in good agreement with their density and porosity [39].

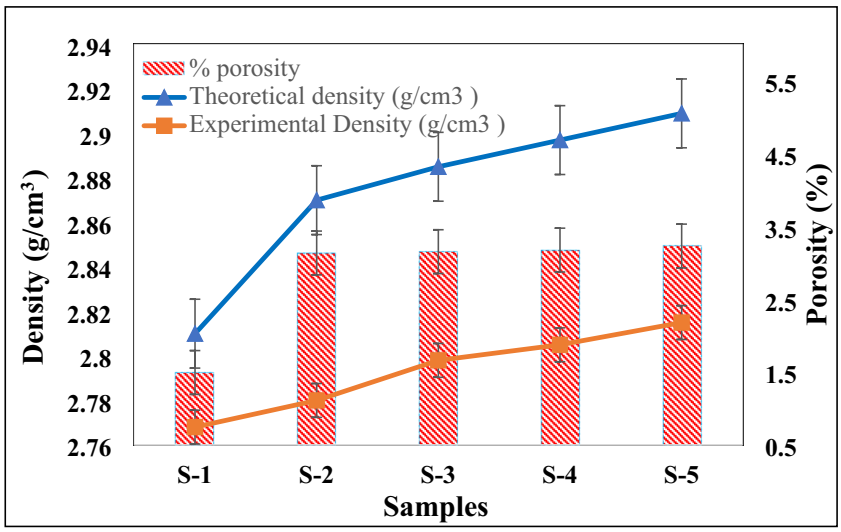

Fig. 4 Experimental and theoretical density with porosity of hybrid aluminium alloy composites

3.2 Microstructure

Figure 5 represents the SEM images of AA7075 alloy (S-1), AA7075 + 6wt. % of SiC + 3 wt. % of TiB_2 (S-3), and AA7075 + 6 wt. % of SiC + 3 wt. % of TiB_2 (S-5) hybrid composite. MMCs reinforced with SiC and TiB_2 particles can be seen in SEM images of synthetic hybrid aluminium composites. The microstructure of AA7075 alloy and their hybrid composite are shown in Fig. 5(a), (b) and (c) which indicate that SiC and TiB_2 reinforced particle present in hybrid aluminium matrix composites. The AA7075/SiC/TiB_2 microstructure conforms to a homogeneous particle dispersion on the molten matrix. Figure 6 shows the higher magnification SEM images (2000x) of both unreinforced and reinforced hybrid composite. It has been observed from Fig. 6 that the Strong interface bonds in hybrid composite compared to unreinforced AA7075 alloy. The strength of the interface bond plays a major role in the transfer of loads between the matrix and reinforcement. To transfer loads between reinforcement particles and matrix, interface bond strength is crucial [40]. The dispersion of SiC and TiB_2 particles prevents motion due to the dislocation of the particles. It also helps to improve the mechanical strength of the hybrid composite. Microstructure also reveals that there is proper interfacial bonding between the reinforcing particles and the alloy matrix. Microstructure of composites displays distribution of two reinforcing particles SiC and TiB_2 with some particle clustering and good interfacial bonding (Fig. 6) However, no porosity is noticed. Sometimes, moderate interfacial reaction is required to bind the reinforcing particle with the matrix which results in enhanced interfacial bonding. Consequently, improved mechanical properties are achieved.

Figure 7(a–c) illustrates the microstructure and EDS spectra at three distinct places for hybrid composite S-2). It can be seen from Fig. 7(a) that the matrix is made of zinc, copper and magnesium as major allowing element (Al-Zn-Cu alloy) containing Si, Ti as minor alloying element. Titanium (Ti) is present in the EDS due to the TiB_2 reinforcement in the matrix material. SiC and TiB_2 were present throughout the hybrid composite, as shown in Fig. 7(b) and (c). Hybrid AA7075 composites showed strong intermolecular bonds between the reinforcement particles and the matrix in the EDS spectrum. A mapping of elemental composition for S-2 at the interfacial position of the matrix and reinforcement is shown in Fig. 8.

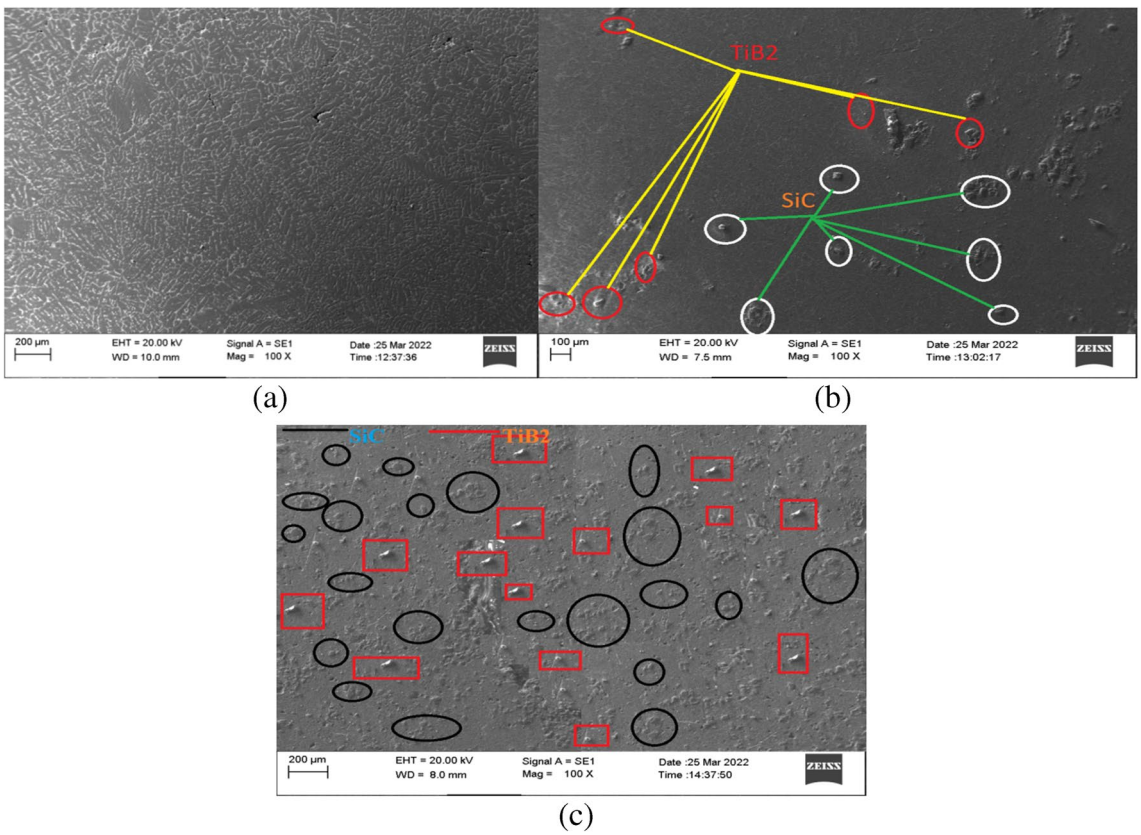

Fig. 5 Scanning electron images (SE mode) (**a**) S-1 (**b**) S-3 (**c**) S-5

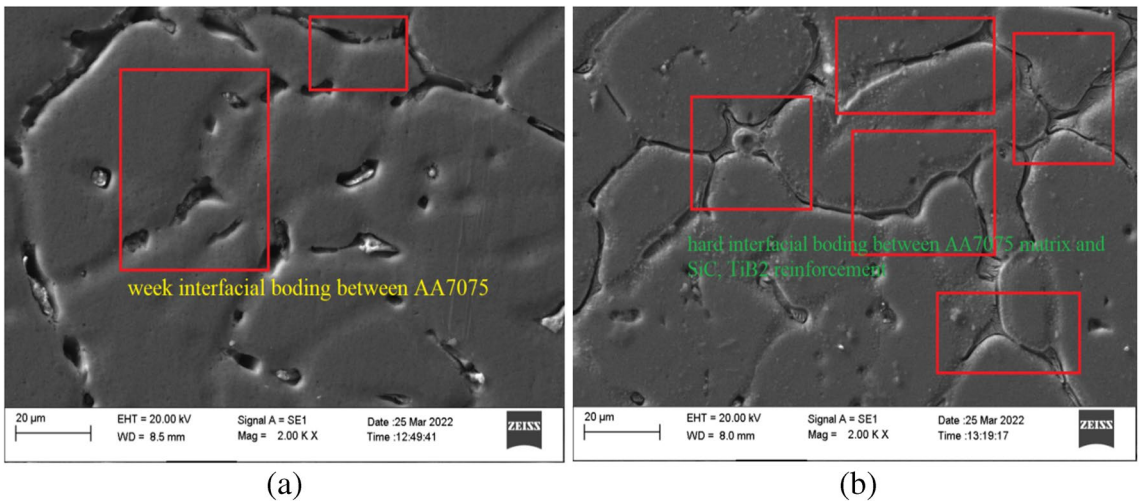

Fig. 6 Higher magnification Scanning electron images (SE mode) (**a**) S-1 (**b**) S-3

3.3 Tensile Strength

The mechanical properties of the AA7075 and its hybrid composite reinforced with 0, 3, 6, 9, and 12 wt. % SiC and 3 wt. % TiB_2 ceramic particles were determined to employ ultimate tensile strength (UTS), Yield strength (YS) and elongation percentage, as shown in Figs. 9 and 10. It was observed that ultimate tensile strength and yield strength increased as the content of SiC increased. The yield strength obtained in the range of 321.80–387.25 MPa for AA7075 matrix alloy with the 0–12 wt. % of SiC and 3 wt. % of TiB_2 respectively. The YS of AA7075 hybrid composite S-2, S-3, S-4, and S-5 increased by 8.94%, 13.30%, 15.36% and 20.33% as compared to unreinforced AA7075 alloy, respectively. The ultimate tensile strength was obtained in the range of 335.8–409.23 MPa

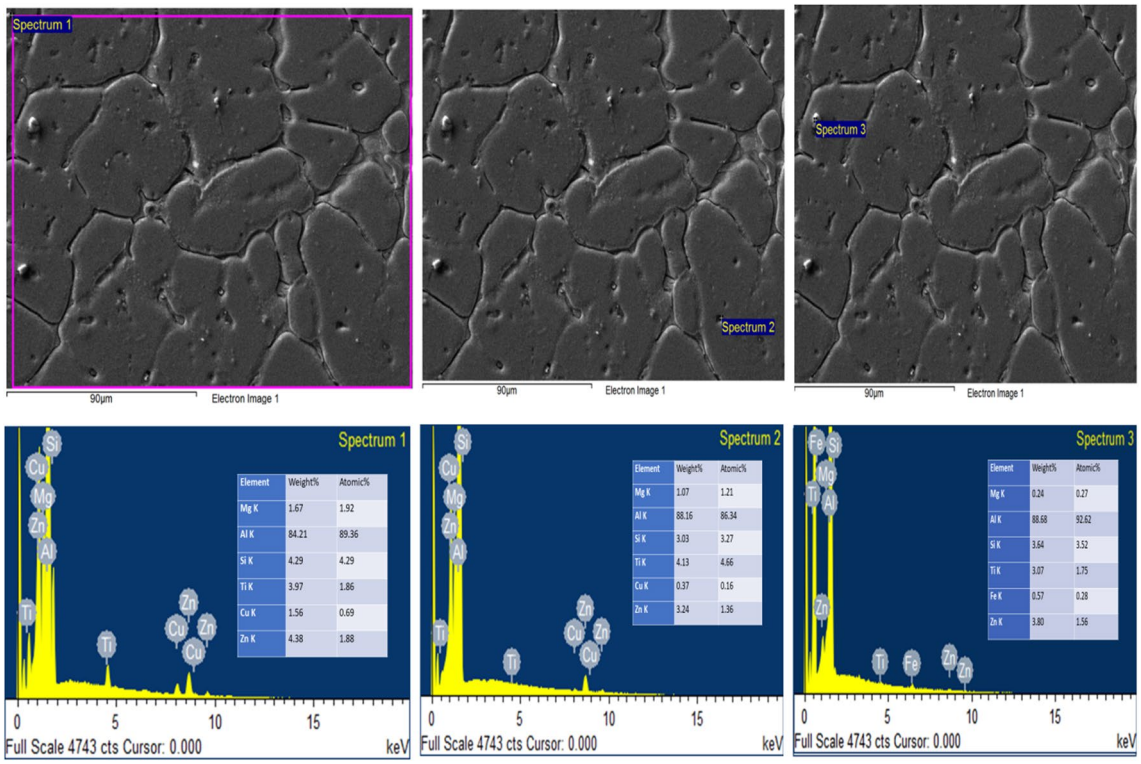

Fig. 7 EDS analysis at various regions of the properly wetted SiC and TiB_2 with AA7075 matrix

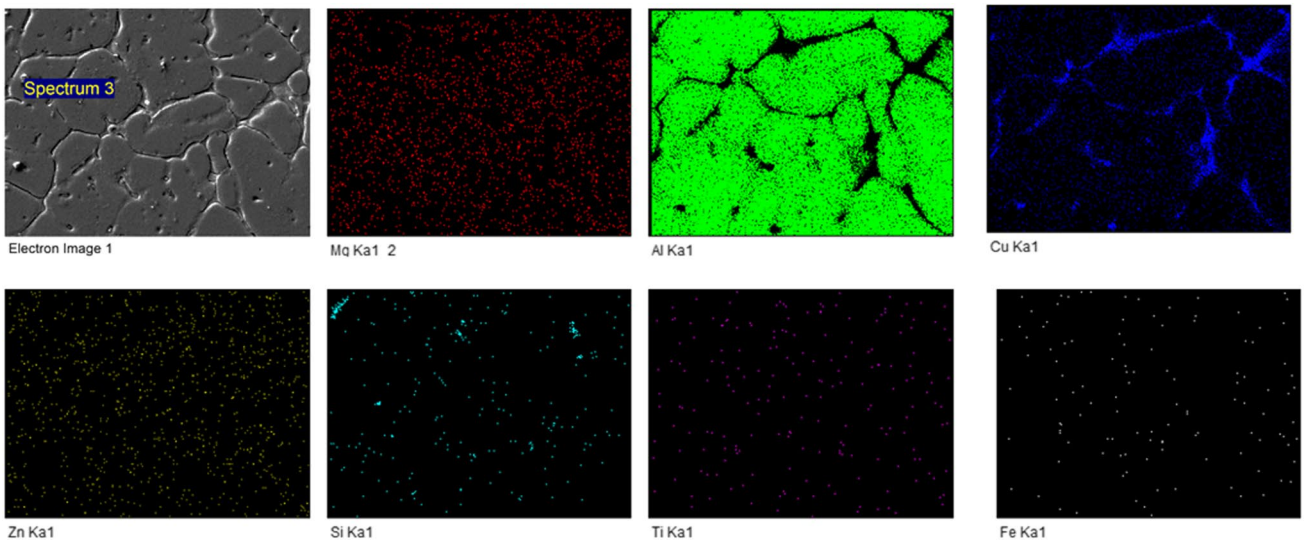

Fig. 8 Mapping of elemental composition for S-2

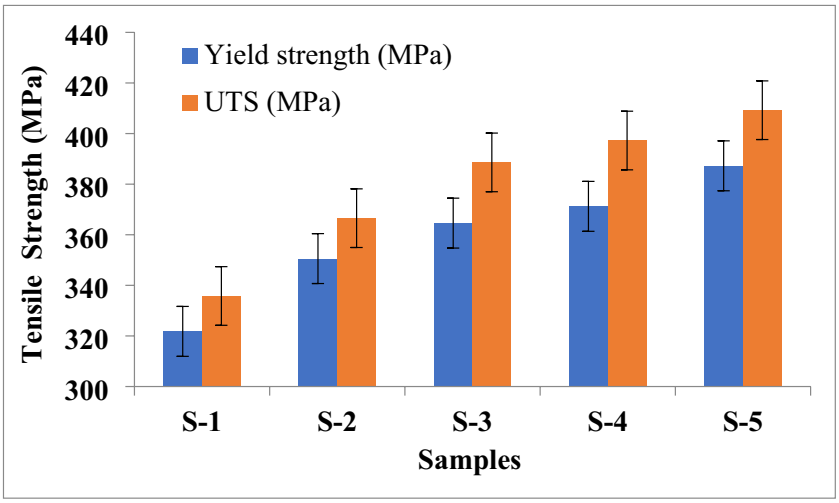

Fig. 9 Tensile properties of AA7075/SiC/TiB_2 hybrid composite

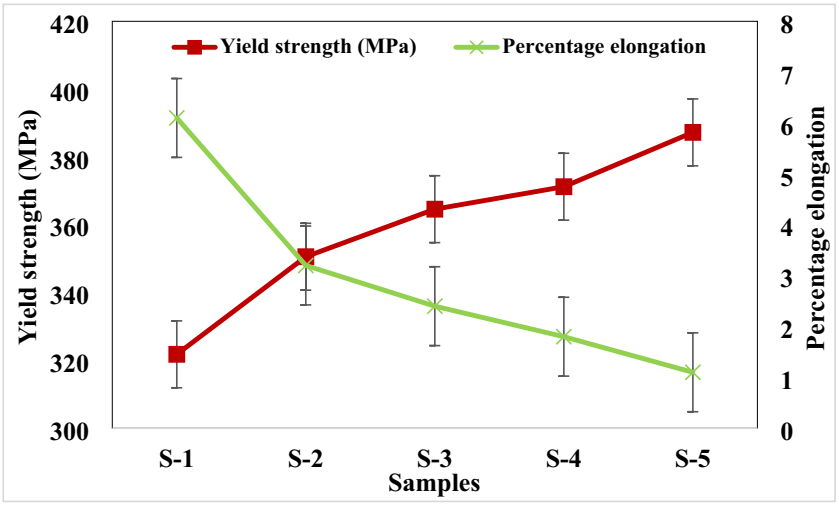

Fig. 10 UTS and percentage of elongation of AA7075/SiC/TiB_2 hybrid composite

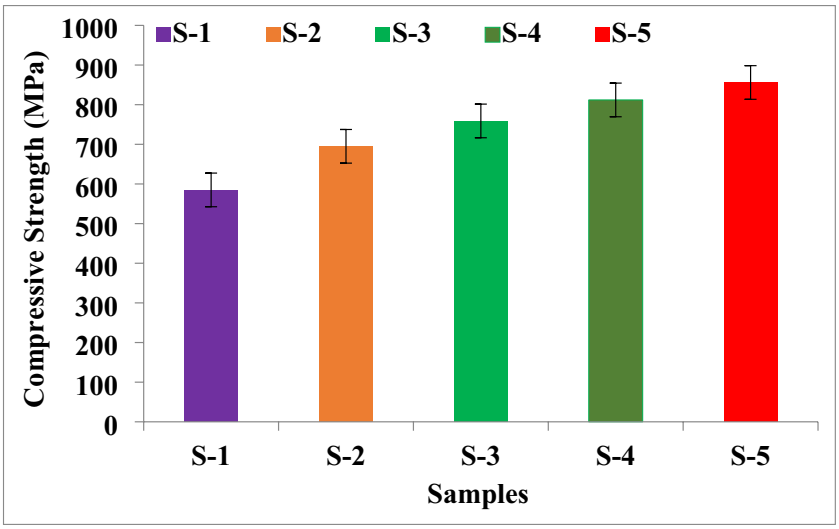

Fig. 11 Compressive strength of AA7075/SiC/TiB_2 hybrid composite

for AA7075 matrix alloy with the 0–12 wt. % SiC and 3 wt. % TiB_2 respectively. The UTS of AA7075 hybrid composite S-2, S-3, S-4, and S-5 increased by 9.15%, 15.72%, 18.29% and 21.86% as compared to unreinforced AA7075 alloy, respectively. The percentage of elongation of AA7075 hybrid composite decreased with the addition of reinforcement SiC and TiB_2. From Fig. 10, the elongation percentage was obtained in a range of 1.1–6.1% for the AA7075 matrix with the 12–0 wt. % SiC and 3 wt. % TiB_2 respectively. The lowest elongation percentage was obtained at AA7075 reinforced with 12 wt. % SiC and 3wt. % TiB_2. The increase in tensile properties like YS, UTS and decrease in ductility with the increase in the amount of reinforcement is due to the SiC and TiB_2 particles in the AA7075 matrix. The SiC particles developed a very strong interfacial boding between aluminium matrix composite [41]. These reinforcement particles refine the grains during solidification and make a hard interfacial bonding between the AA7075 matrix and SiC, TiB_2 reinforcement. The interfacial bonding resistance to the motion of dislocation in the AA7075/SiC/TiB_2 hybrid composites than the AA7075 alloy also transfers the load from the matrix to the reinforcements. Enhanced tensile strength typically results from grain refinement, combined with direct and indirect strengthening. The hybrid composite benefits from the supportive nature of SiC and TiB_2 particles, contributing to its increased strength. The incorporation of reinforcement leads to enhanced YS and UTS, attributed to the even dispersion of SiC and TiB_2, as confirmed by SEM images. The tensile properties of hybrid composites are significantly influenced by mechanical alloying and the uniform dispersion of SiC and TiB_2 within the AA7075 matrix.

3.4 Compressive Strength

Figure 11 shows the compression test result for the fabricated AA7075/SiC/TiB2 hybrid composites reinforced with 0, 3, 6, 9, and 12 wt. % SiC and 3 wt. % TiB_2 ceramic particles. The

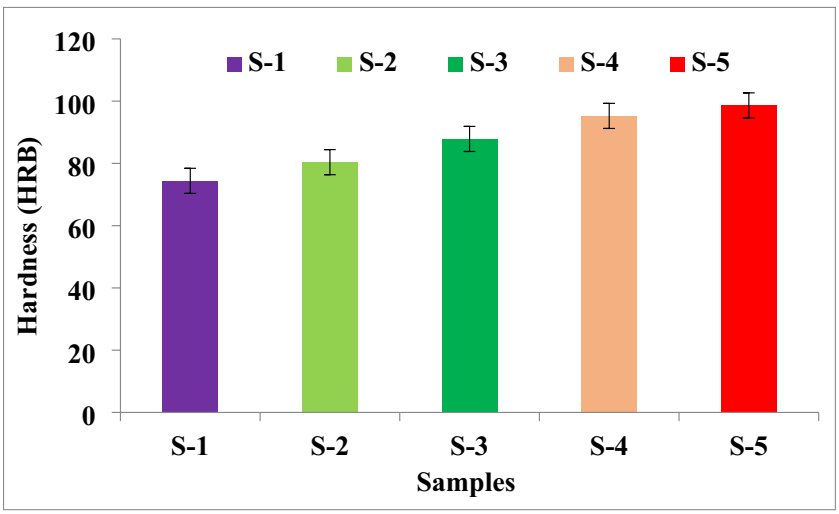

Fig. 12 Harness value AA7075/SiC/TiB_2 hybrid composite

compressive strength obtained in the range of 585 to 856 MPa for AA7075 matrix alloy with the 0–12 wt. % of SiC and 3 wt. % of TiB_2 respectively. The compressive strength of AA7075 hybrid composite S-2, S-3, S-4, and S-5 increased by 18.80%, 29.74%, 38.80% and 46.32% as compared to unreinforced AA7075 alloy, respectively. The Compressive strength of AA7075/SiC/TiB_2 hybrid composite is increased with the addition of reinforcement particle SiC and TiB_2. Improvement in compressive strength with addition of reinforcement particle SiC and TiB_2 in AA7075 is due to effective load transfer and grain refinement as seen in microstructure. Another reason is the uniform distribution of SiC and TiB_2 which hinders dislocation movement and strengthening of grain boundaries.

3.5 Hardness

Figure 12 shows the Rockwell hardness values for the fabricated hybrid composites reinforced with 0, 3, 6, 9, and 12 wt. % SiC and 3 wt. % TiB_2 ceramic particles. The hardness values obtained in the range of 74.4 to 98.6 HRB for AA7075 matrix alloy with the 0–12 wt. % SiC and 3

Table 4 Comparative study of mechanical properties of aluminium composites

Material	Composition	Technique	YS (MPa)	UTS (MPa)	% of Elongation	Compressive strength (MPa)	Hardness	
AA7075	AA7075	Stir casting		141.90	8.07		75HV	[3]
	AA7075 + 6wt% TiB_2			219.67	4.9		101HV	
	AA7075 + 9wt% TiB_2			250.70	3.2		125HV	
	AA7075 + 12wt% TiB_2			279.91	2.9		141HV	
Al7075	Al7075	Stir casting	109.32	116.91	2.16		110 HV	[4]
	Al7075 + 2% TiB_2		131.60	138.26	1.98		137 HV	
	Al7075 + 4% TiB_2		147.95	155.99	1.58		174 HV	
	Al7075 + 6% TiB_2		172.86	183.89	1.34		182 HV	
	Al7075 + 8% TiB_2		211.89	227.39	0.56		217 HV	
AA7075	AA7075	Stir casting				209		[9]
	AA7075 + 3%Flyash + 2.5% TiO_2					312		
	AA7075 + 3%Flyash + 5% TiO_2					373		
	AA7075 + 3%Flyash + 7.5% TiO_2					412		
	AA7075 + 3%Flyash + 10% TiO_2					421		
Al7075	Al7075	Stir casting	441.02	504.80			175VHN	[17]
	Al7075 + 2.5%FA + 2.5%SiC		445.09	511.58			178 VHN	
	Al7075 + 5%FA + 2.5%SiC		453.23	512.94			183 VHN	
	Al7075 + 7.5%FA + 2.5%SiC		458.66	517.01			188 VHN	
	Al7075 + 10%FA + 2.5%SiC		502.08	526.15			195 VHN	
Al7075	Al7075	Stir casting		140	3.09		66 HV	[23]
	Al7075 + 7 wt.% of SiC			192	1.90		82 HV	
	Al7075 + 7 wt.% of TiB_2			198	1.70		86HV	
AA7075	AA7075	Stir casting		210		265	115 BHN	[29]
	AA7075/2% Al2O3			219		270	117 BHN	
	AA7075/4% Al2O3			226		275	121 BHN	
	AA7075/6% Al2O3			229		283	124 BHN	
	AA7075/8% Al2O3			236		294	134 BHN	
Al7075	Al7075	Stir–squeeze casting		221		485	60 VHN	[39]
	Al7075 + 3% B_4C			286		633.6	127.4 VHN	
	Al7075 + 6% B_4C			296		723.8	145.6 VHN	
	Al7075 + 9% B_4C			313		759	159.9 VHN	
	Al7075 + 3% B_4C + 3% BN			322		653.8	143 VHN	
	Al7075 + 6% B_4C + 3% BN			355		786.77	158.6 VHN	
	Al7075 + 9% B_4C + 3% BN			368		833.96	171 VHN	

Table 4 (continued)

Material	Composition	Technique	YS (MPa)	UTS (MPa)	% of Elongation	Compressive strength (MPa)	Hardness	
AA7075	AA7075	Sintered through conventional technique		112		185	69 HV	[43]
	AA7075 + 1% SiC			125		198	79 HV	
	AA7075 + 2% SiC			152		220	82 HV	
	AA7075 + 3% SiC			190		240	85 HV	
	AA7075 + 4% SiC			230		280	87 HV	
	AA7075 + 5% SiC			270		323	89 HV	
	AA7075 + 6% SiC			295		351	95 HV	
	AA7075 + 7% SiC			323		382	96 HV	
	AA7075 + 8% SiC			315		375	96 HV	
	AA7075 + 9% SiC			289		350	98 HV	
	AA7075 + 10% SiC			260		322	101 HV	
	AA7075 + 7% SiC + 1% Graphite			329		402	96 HV	
	AA7075 + 7% SiC + 2% Graphite			335		415	99 HV	
	AA7075 + 7% SiC + 3% Graphite			342		429	103 HV	
	AA7075 + 7% SiC + 4% Graphite			359		432	106 HV	
	AA7075 + 7% SiC + 5% Graphite			365		451	109 HV	
	AA7075 + 7% SiC + 6% Graphite			341		421	109 HV	
	AA7075 + 7% SiC + 7% Graphite			315		389	110 HV	
Al7075	Al7075	Two-stage stir casting		188			110 BHN	[44]
	Al7075 + 10% cow dung ash (CDA)			230			103 BHN	
	Al7075 + 2.5% B_4C + 7.5% CDA			250			119 BHN	
	Al7075 + 2.5% B_4C + 5% CDA			268			132 BHN	
	Al7075 + 2.5% B_4C + 2.5% CDA			290			144 BHN	
	Al7075 + 10% B_4C			274			152 BHN	
Al7075	Al7075		95	221	6.2		60 VHN	[45]
	Al7075 + 4% B_4C + 3% MoS_2		123.42	268.21	4.8		72.5 VHN	
	Al7075 + 8% B_4C + 3% MoS_2		137.50	281.32	4.1		88.6 VHN	
	Al7075 + 12% B_4C + 3% MoS_2		172.60	298.52	3.7		94.32 VHN	
AA7075	AA7075	Stir casting		236.29	9.91		61.40 HRB	[46]
	AA7075 + 5% SiC			259.63	7.74		70.64 HRB	
	AA7075 + 5% SiC + 3% RHA			271.36	10.4		79.47 HRB	
	AA7075 + 5% SiC + 3% RHA + 1% CES			289.26	5.96		81.73 HRB	

Table 4 (continued)

Material	Composition	Technique	YS (MPa)	UTS (MPa)	% of Elongation	Compressive strength (MPa)	Hardness	
AA7075	AA7075	Top loaded bottom pouring stir casting	321.8	335.8	6.1	585	74.4 HRB	Self
	AA7075 + 3 wt. % SiC + 3wt. % TiB_2		350.58	366.55	3.2	695	80.4 HRB	
	AA7075 + 6 wt. % SiC + 3wt. % TiB_2		364.6	388.58	2.4	759	87.86 HRB	
	AA7075 + 9 wt. % SiC + 3wt. % TiB_2		371.23	397.25	1.8	812	95.26 HRB	
	AA7075 + 12 wt. % SiC + 3wt. % TiB_2		387.25	409.23	1.1	856	98.63 HRB	

wt. % TiB_2 respectively. The hardness of AA7075 hybrid composite S-2, S-3, S-4, and S-5 increased by 8.064%, 18.091%, 28.03% and 32.56% as compared to unreinforced AA7075 alloy, respectively. The hardness of AA7075/SiC/TiB_2 hybrid composite was increased with the addition of reinforcement particles SiC and TiB_2 because reinforcements SiC and TiB_2 have higher hardness values than AA7075 (Matrix alloy) which contributes to the increase in the hardness of fabricated hybrid composites which is a similar to the past literature [42]. It was also observed that the increase in hardness of fabricated hybrid composite is due to the resistance to the motion of dislocation in the AA7075/SiC/TiB_2 hybrid composites than the AA7075 alloy as well as the addition of reinforcement enhances the intermetallic bonding between matrix and reinforcement. Karpasand et al. [36] showed that matrix and reinforcement particles share the indenter load during the hardness test, which increases hardness. Reinforcement with SiC and TiB_2 particle improve all mechanical properties as shown in Table 4.

3.6 Wear Behavior

At five sliding distances, 1000 m, 2000 m, 3000 m, 4000 m, and 5000 m at constant sliding velocity, and under three loading conditions, viz 2 kg, 4 kg, and 6 kg, composites with 0, 3, 6, 9 and 12 wt. % reinforcement of SiC and 3 wt. % TiB_2 were examined. The wear track diameter was taken as 100 mm for all test samples to determine the wear rate (mm^3/m). Using Eq. 3, the wear rate of samples was evaluated by measuring the difference between their weights before and after testing. Figure 13 shows wear rates of cast AA7075 alloy and its hybrid composites with SiC and TiB_2 particles as a function of various applied loads (2, 4, and 6 kg) and sliding distances (1000 m). The wear rate of AA7075 alloy and its hybrid composites increases with the load applied due to the frictional forces between the composite surface and the counter surface (disk) increasing at the interface. However, the wear rate of AA7075 alloy was noticed as higher than hybrid reinforced composites due to frictional forces during the sliding. Increasing the

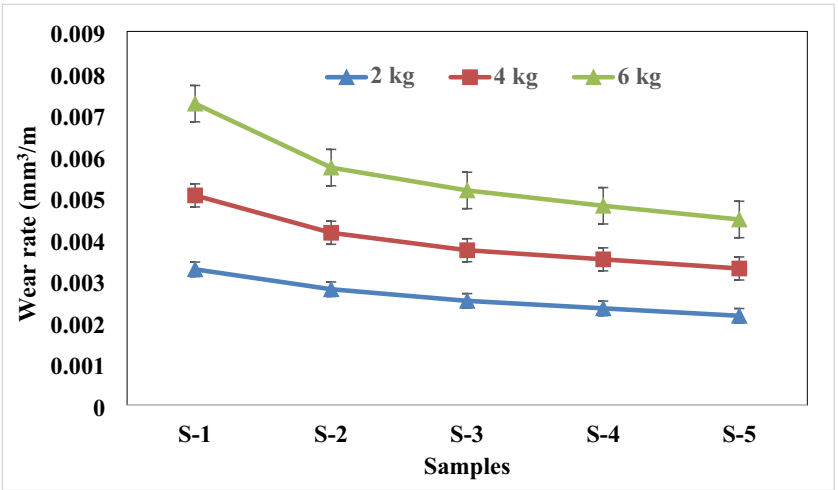

Fig. 13 Wear rate of cast AA7075/SiC/TiB_2 hybrid composite hybrid composites constant sliding speed (1.7 m/s) and sliding distance (1000 m)

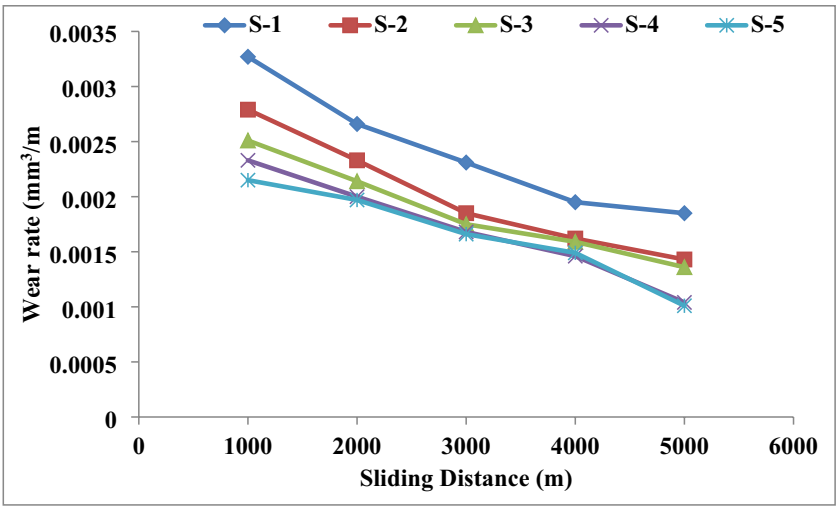

Fig. 14 Wear rate under the influence of sliding distance on AA7075/SiC/TiB_2 hybrid composites

applied load causes a rise in temperature at the composites' interfaces, reducing their hardness and wear resistance. The wear rate of AA7075/SiC/TiB_2 hybrid composites was significantly reduced by adding SiC and TiB_2 particles as reinforcement. As a result of the homogenous distribution and addition of SiC and TiB_2 reinforcement particles in AA7075, the reinforcement particles form a strong bond, increasing the hardness and protecting the surface against wear. It can clearly see from the SEM images that the grains of the matrix alloy are getting refined with the addition of reinforcing particles (SiC and TiB_2) into the matrix which results in increasing the grain boundary concentration and finally turns into increase in wear resistance properties. Composite specimens were ordered from best to worst by the level of wear performance: S-5 > S-4 > S-3 > S-2 > S-1.

The wear properties of AA7075 alloy and its hybrid composites reinforced with SiC (0, 3, 6, 9 and 12 wt. %) and of TiB_2 (3 wt. %) as a function of sliding distance (1000, 2000, 3000, 4000 rpm and 5000 m) at an applied load of 2 kg and sliding speed (1.7 m/s) as depicted in Fig. 14. Results indicate the wear rate is inversely proportional to the sliding distance and the addition of SiC reinforcement particles. SiC/TiB_2 hybrid reinforced composites showed better wear resistance when compared to unreinforced AA7075 at various sliding distances.

4 Conclusion

AA7075 alloy and AA7075 + SiC + TiB_2 hybrid composites reinforced with 0, 3, 6, 9, and 12 wt. % of SiC with particle size 25 µm and 3 wt. % of TiB_2 with particle size 15 µm were fabricated by top loaded bottom pouring stir casting method. The Microstructure of AA7075 alloy (unreinforced matrix material) shows SiC and TiB_2 reinforced aluminium matrix composites display the homogeneous type of particle dispersion on the entire molten matrix. The addition of reinforcement particles SiC + 3 wt. % of TiB_2 in AA7075 alloy caused a significant increase in yield strength (321.8 MPa to 387.25 MPa), ultimate tensile strength (335.8 MPa to 409.23 MPa), compressive strength (585 MPa to 856 MPa) and hardness values. Improvement in mechanical characteristics with the addition of reinforcement particle SiC and TiB_2 in AA7075 is due to effective load transfer and grain refinement as seen in the microstructure. The higher wear resistance of the reinforced AA7075 alloy was found with 12 wt. % SiC and 3 wt. % of TiB_2 particles with varying the sliding distance at a constant applied load of 2 kg and sliding speed of 1.7 m/s due to the homogenous distribution of the SiC and TiB_2 reinforced particle.

Acknowledgements The authors gratefully acknowledge the present work as part of research work funded by VIT Bhopal University under Support for Excellence in Academic Research (SPEAR) grant number SMG-01.

Authors' Contribution **NKS**: Fabrication, testing, Investigation, Resources, and Writing—original draft.
BS: Conceptualization, Supervision, Writing—review & editing.

Funding This work was supported by VIT Bhopal University under Support for Excellence in Academic Research (SPEAR) grant number SMG-01.

Data Availability All data sources are described in this study are directed at the author.

Declarations

The Authors declare that they don't have known personal relationships or competing financial interest that could have appeared to influence the work reported in this manuscript.

Competing interests The authors declare no competing interests.

Ethics Approval No ethical issues arose during either the experimental process or the preparation of the manuscript.

Research Involving Human Participants and/or Animals Not applicable.

Informed Consent Not applicable.

Consent to Participate All the Authors are happily agreeing to contribute in this research work.

Consent for Publication All authors have given their consent to publish this manuscript.

Conflict of Interest The authors declare that they have no conflict of interest.

References

1. Rao CM, Mallikarjuna Rao K (2018) Abrasive wear behaviour of TiB2 fabricated aluminum 6061. Mater Today Proc 5(1):268–275. https://doi.org/10.1016/j.matpr.2017.11.082
2. Singh N, Mir IUH, Raina A, Anand A, Kumar V, Sharma SM (2018) Synthesis and tribological investigation of Al-SiC based nano hybrid composite. Alex Eng J 57(3):1323–1330. https://doi.org/10.1016/j.aej.2017.05.008
3. Sethi D, Kumar S, Choudhury S, Shekhar S, Saha B (2020) Synthesis and characterization of AA7075/TiB2 aluminum matrix composite formed through stir casting method. Mater Today Proc 26:1908–1913. https://doi.org/10.1016/j.matpr.2020.02.418
4. Manoj M, Jinu GR, Kumar JS, Mugendiran V (2021) Effect of TiB2 particles on the morphological, mechanical and corrosion behaviour of Al7075 metal matrix composite produced using stir casting process. Int J Met 16(3):1517–1532. https://doi.org/10.1007/s40962-021-00696-3
5. Bommana D, Dora TRK, Senapati NP, Kumar AS (2021) Effect of 6 Wt.% particle (B4C + SiC) reinforcement on mechanical properties of AA6061 aluminum hybrid MMC. Silicon 1:4197–4206. https://doi.org/10.1007/s12633-021-01210-4
6. Ko S et al (2020) Fabrication of TiB2-Al1050 composites with improved microstructural and mechanical properties by a liquid pressing infiltration process. Materials (Basel) 13(7). https://doi.org/10.3390/ma13071588
7. Muniappan A, Vamsikrishna B, Charankumar RG, et al (2015) Fabrication of hybrid aluminium composite using stir casting method. Int J Appl Eng Res 10:38–43
8. Balaji V, Sateesh N, Hussain MM (2015) Manufacture of aluminium metal matrix composite (Al7075-SiC) by stir casting technique. Mater Today Proc 2(4–5):3403–3408. https://doi.org/10.1016/j.matpr.2015.07.315
9. Shivananda Murthy KV, Girish DP, Keshavamurthy R, Varol T, Koppad PG (2017) Mechanical and thermal properties of AA7075/TiO2/Fly ash hybrid composites obtained by hot forging. Prog Nat Sci Mater Int 27(4):474–481. https://doi.org/10.1016/j.pnsc.2017.08.005
10. Yuvaraj N, Aravindan S (2015) Fabrication of Al5083 / B 4 C surface composite by friction stir processing and its tribological characterization. Integr Med Res 4(4):398–410. https://doi.org/10.1016/j.jmrt.2015.02.006
11. Zayed EM, Ahmed MMZ, Rashad RM (2019) Development and characterization of AA5083 reinforced with SiC and Al 2 O 3 particles by friction stir processing. Springer International Publishing
12. Manohar G, Pandey KM, Maity SR (2021) Effect of microwave sintering on the microstructure and mechanical properties of AA7075/B4C/ZrC hybrid nano composite fabricated by powder metallurgy techniques. Ceram Int 47(23):32610–32618. https://doi.org/10.1016/j.ceramint.2021.08.156
13. Ravikumar LVTVAK (2019) Microstructural characteristics and mechanical behaviour of aluminium hybrid composites reinforced with groundnut shell ash and B 4 C. J Braz Soc Mech Sci Eng 41(7):1–13. https://doi.org/10.1007/s40430-019-1800-1
14. Prema CE, Suresh S, Ramanan G, Sivaraj M (2020) Characterization, corrosion and failure strength analysis of Al7075 influenced with B4C and Nano-Al2O3 composite using online acoustic emission. Mater Res Express 7:16524. https://doi.org/10.1088/2053-1591/ab6257
15. Sreedhar N, Balaguru S (2020) Mechanical and tribological behaviour of al 7075 hybrid mnc's using stir casting method. Int J Mech Prod Eng Res Dev 10(3):391–400. https://doi.org/10.24247/ijmperdjun202036
16. Mohanavel V, Kumar SS, Sathish T, Adithiyaa T, Mariyappan K (2018) ScienceDirect Microstructure and mechanical properties of hard ceramic particulate reinforced AA7075 alloy composites via liquid metallurgy route. Mater Today Proc 5(13):26860–26865. https://doi.org/10.1016/j.matpr.2018.08.168
17. Mandava RK, Reddy VV, Rao VRK, Reddy KS (2021) Wear and frictional behaviour of Al 7075/FA/SiC hybrid MMC's using response surface methodology. SILICON. https://doi.org/10.1007/s12633-021-01300-3
18. Bhushan RK, Kumar S, Das S (2013) Fabrication and characterization of 7075 Al alloy reinforced with SiC particulates. Int J Adv Manuf Technol 65(5–8):611–624. https://doi.org/10.1007/s00170-012-4200-6
19. Sahu MK, Sahu RK (2020) Experimental investigation, modeling, and optimization of wear parameters of B4C and fly-ash reinforced aluminum hybrid composite. Front Phys 8(July):1–14. https://doi.org/10.3389/fphy.2020.00219
20. Umanath K, Palanikumar K, Selvamani ST (2013) Analysis of dry sliding wear behaviour of Al6061/SiC/Al2O 3 hybrid metal matrix composites. Compos Part B Eng 53:159–168. https://doi.org/10.1016/j.compositesb.2013.04.051
21. Bin Li A, Xu HY, Geng L, Li BL, Bin Tan Z, Ren W (2012) Preparation and characterization of SiC p/2024Al composite foams by powder metallurgy. Trans Nonferrous Met Soc China (English Ed) 22(SUPPL. 1):33–38. https://doi.org/10.1016/S1003-6326(12)61680-X
22. Suresh S, Natarajan E, Shanmugam R, Venkatesan K, Saravanakumar N, AntoDilip A (2022) Strategized friction stir welded AA6061-T6/SiC composite lap joint suitable for sheet metal applications. J Mater Res Technol 21:30–39. https://doi.org/10.1016/j.jmrt.2022.09.022
23. Bhowmik A, Dey D, Biswas A (2021) Characteristics Study of Physical, Mechanical and Tribological Behaviour of SiC/TiB2 Dispersed Aluminium Matrix Composite. Silicon 1133–1146. https://doi.org/10.1007/s12633-020-00923-2
24. Chen Y, Jian Z, Ren Y, Li K, Dang B, Guo L (2023) Influence of TiB2 volume fraction on SiCp/AlSi10Mg composites by LPBF: microstructure, mechanical, and physical properties. J Mater Res Technol 23:3697–3710. https://doi.org/10.1016/j.jmrt.2023.02.031
25. Fenghong C, Chang C, Zhenyu W, Muthuramalingam T, Anbuchezhiyan G (2019) Effects of silicon carbide and tungsten carbide in aluminium metal matrix composites. SILICON 11(6):2625–2632. https://doi.org/10.1007/s12633-018-0051-6
26. Suresh S, Venkatesan K, Natarajan E (2018) Influence of SiC Nanoparticle Reinforcement on FSS Welded 6061–T6 Aluminum Alloy. J Nanomater 2018:7031867. https://doi.org/10.1155/2018/7031867

27. Singh NK, Balaguru S (2023) Experimental analysis of foaming agent contents in AA7075/SiC closed cell aluminum composite foam BT - recent advances in mechanical engineering. In: Sethuraman B, Jain P, Gupta M (eds). Springer Nature Singapore, Singapore, pp 567–575. https://doi.org/10.1007/978-981-99-2349-6_51
28. Rathore RK, Singh NK, Xavier JF (2021) Characterization of AA7075 alloy foam using calcium and magnesium carbonate as foaming agent BT - processing and characterization of materials: Select proceedings of CPCM 2020. In: Pal S, Roy D, Sinha SK (eds). Springer Singapore, Singapore, pp 289–297. https://doi.org/10.1007/978-981-16-3937-1_30
29. Imran M, Khan ARA (2019) Characterization of Al-7075 metal matrix composites: a review. J Mater Res Technol 8(3):3347–3356. https://doi.org/10.1016/j.jmrt.2017.10.012
30. Sunar T, Tuncay T, Özyürek D, Gürü M (2020) Investigation of mechanical properties of AA7075 alloys aged by various heat treatments. Phys Met Metallogr 121(14):1440–1446. https://doi.org/10.1134/S0031918X20140161
31. Johny James S, Venkatesan K, Kuppan P, Ramanujam R (2014) Comparative study of composites reinforced with SiC and TiB 2. Procedia Eng 97:1012–1017. https://doi.org/10.1016/j.proeng.2014.12.378
32. Khairaldien WM, Khalil AA, Bayoumi MR (2007) Production of aluminum-silicon carbide composites using powder metallurgy at sintering temperatures above the aluminum melting point. J Test Eval 35(6):655–667. https://doi.org/10.1520/jte100677
33. Chandla NK, Yashpal, Kant S, Goud MM, Jawalkar CS (2020) Experimental analysis and mechanical characterization of Al 6061/alumina/bagasse ash hybrid reinforced metal matrix composite using vacuum-assisted stir casting method. J Compos Mater 54(27):4283–4297. https://doi.org/10.1177/0021998320929417
34. Rathore RK, Singh NK, Sinha AK, Panthi SK, Sharma AK (2022) Mechanical properties of lightweight aluminium hybrid composite foams (AHCFs) for structural applications. Adv Mater Process Technol 8(4):4194–4208. https://doi.org/10.1080/2374068X.2022.2048498
35. Dey D, Bhowmik A, Biswas A (2021) Characterization of physical and mechanical properties of aluminium based composites reinforced with titanium diboride particulates. J Compos Mater 55(14):1979–1991. https://doi.org/10.1177/0021998320980800
36. Karpasand F, Abbasi A, Ardestani M (2020) Effect of amount of TiB2 and B4C particles on tribological behavior of Al7075/B4C/TiB2 mono and hybrid surface composites produced by friction stir processing. Surf Coat Technol. 390(19):125680. https://doi.org/10.1016/j.surfcoat.2020.125680
37. Sinha AK, Narang HK, Bhattacharya S (2021) Experimental determination, modelling and prediction of sliding wear of hybrid polymer composites using RSM and fuzzy logic. Arab J Sci Eng 46(3):2071–2082. https://doi.org/10.1007/s13369-020-04997-3
38. Singh NK, Sethuraman B (2023) Development and characterization of Aluminium AA7075 hybrid composite foams (AHCFs) using SiC and TiB2 Reinforcement. Int J Met. https://doi.org/10.1007/s40962-023-01009-6
39. Ramadoss N, Pazhanivel K, Ganeshkumar A, Arivanandhan M (2023) Microstructural, mechanical and corrosion behaviour of B4C/BN-reinforced Al7075 matrix hybrid composites. Int J Met 17:499–514. https://doi.org/10.1007/s40962-022-00791-z
40. Thamilarasan J, Karthik K, Balaguru S, et al (2023) An investigation on the mechanical properties of graphene nanocomposite BT - recent advances in mechanical engineering. In: Sethuraman B, Jain P, Gupta M (eds). Springer Nature Singapore, Singapore, pp 483–492. https://doi.org/10.1007/978-981-99-2349-6_44
41. Venugopal S, Karikalan L (2020) Microstructure and physical properties of hybrid metal matrix composites AA6061-TiO2-SiC via stir casting techniques. Mater Today Proc 37(Part 2):1289–1294. https://doi.org/10.1016/j.matpr.2020.06.462
42. Balaguru S, Kumar KN, Natarajan E (2018) Experimental and numerical investigation on mechanical properties of AA6061T6 reinforced with SiC and Al2O3. Int J Mech Prod Eng Res Dev 201–206
43. Manohar G, Pandey KM, Maity SR (2022) Effect of variations in microwave processing temperatures on microstructural and mechanical properties of AA7075/SiC/graphite hybrid composite fabricated by powder metallurgy techniques. Silicon 14:7831–7847. https://doi.org/10.1007/s12633-021-01554-x
44. Manikandan R, Arjunan TV (2020) Studies on micro structural characteristics, mechanical and tribological behaviours of boron carbide and cow dung ash reinforced aluminium (Al 7075) hybrid metal matrix composite. Compos Part B Eng 183:107668. https://doi.org/10.1016/j.compositesb.2019.107668
45. Liu S, Wang Y, Muthuramalingam T, Anbuchezhiyan G (2019) Effect of B 4 C and MOS 2 reinforcement on micro structure and wear properties of aluminum hybrid composite for automotive applications. Compos Part B 176(August):107329. https://doi.org/10.1016/j.compositesb.2019.107329
46. Khan AH, Shah SAA, Umar F, et al (2022) Investigating the Microstructural and Mechanical Properties of Novel Ternary Reinforced AA7075 Hybrid Metal Matrix Composite. Materials (Basel) 15. https://doi.org/10.3390/ma15155303